Heliyon 10 (2024) e33011

Contents lists available at ScienceDirect

Heliyon

journal homepage: www.cell.com/heliyon

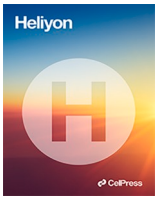

Research article

Relief effect of biochar on continuous cropping of tobacco through the reduction of *p*-hydroxybenzoic acid in soil

Haijun Hu [a,c], Jun Meng [b], Huan Zheng [a], Heqing Cai [a], Maoxian Wang [a], Zhenbao Luo [a], Yang E [a,b,*], Caibin Li [a,**], Qiaoxue Wu [a], Zhiqiang Yan [d], Yue Lei [d]

[a] *Bijie Tobacco Company of Guizhou Province, Bijie, Guizhou, 551700, PR China*
[b] *National Biochar Institute of Shenyang Agricultural University, Shenyang, 110866, PR China*
[c] *Zunyi Normal College, Zunyi, 863002, PR China*
[d] *Guizhou Rice Research Institute, Guiyang, 550016, PR China*

ARTICLE INFO

Keywords:
Tobacco
Biochar
p-hydroxybenzoic acid
Adsorption
Continuous cropping

ABSTRACT

Biochar application to soil has proven to be an excellent approach for decreasing the concentration of auto-toxic compounds and promoting plant growth in continuous-cropping fields. However, the mechanisms underlying the action pathway among biochars, auto-toxic compounds and tobacco remain unknown. In this study, we conducted an experiment tracking the incidence rate of black rot and auto-toxic compounds for a 3-year continuous-cropping tobacco pot trial in response to biochar treatment intensity compared with that of non-biochar treatment. Biochar inhibited the incidence of black rot. Using ultra-high-performance liquid chromatography–mass spectrometry (UPLC–MS/MS), we revealed that biochar can effectively decrease the concentration of *p*-hydroxybenzoic acid (PHA), which is associated with the incidence rate of black rot ($R^2 = 0.890$, $p < 0.05$). The sorption kinetics and isotherm of PHA sorption on biochar indicate that the coexistence of heterogeneous and monolayer sorption plays an important role in the adsorption process. Using Molecular dynamics (MD), Density functional theory (DFT) and Independent gradient model (IGM) analyses, we provide evidence that van der Waals force (vdW), π–π bonds and H-bonds between biochar and PHAs are the dominant factors that affect adsorption capacity. Moreover, the molecular adsorption rate ($N_{biochar}$: N_{PHAs} = 1:4) was theoretically calculated. In contrast, biochar dramatically increased nutrient retention capacity and improved soil properties, further enhancing tobacco quality, including its agronomic and physiological traits. Therefore, we considered that biochar not only relieved continuous cropping but also improved soil properties suitable for tobacco growth. Together, we demonstrate that the action of biochar in continuously cropped soil improves soil traits and alleviates auto-toxic compound toxicity. These data contribute to the direction of modified biochar application to improve continuous-cropping soil.

1. Introduction

In recent years, the widespread adoption of instalment agriculture and the grain industry has led to a growing challenge of

* Corresponding author.
** Corresponding author.
E-mail addresses: eyang@syau.edu.cn (Y. E), ynlcb2015@126.com (C. Li).

https://doi.org/10.1016/j.heliyon.2024.e33011
Received 28 August 2023; Received in revised form 12 June 2024; Accepted 12 June 2024
Available online 15 June 2024

continuous-cropping obstacles in soil [1]. In the past 5 years, numerous studies have identified 3 primary factors contributing to these obstacles: nutritional imbalance, pathogenic bacteria overflow and the accumulation of allelopathic compounds (ACs) leading to auto-toxicity [2–4]. Due to auto-toxicity in rhizosphere soil, the microbial population shifts from probiotics to pathogenic bacteria, leading to an increase in diseases and insect pest incidence [3–6]. Despite the extensive use of chemical agents to overcome continuous-cropping obstacles [7], these incidences remain inadequately suppressed [8]. Furthermore, the surplus of chemical agents in the soil causes groundwater pollution with rainwater leaching and soil compaction [9]. It is a current challenge to relieve continuous-cropping obstacles through a series of green and environmentally friendly approaches.

Allelochemicals are 'organic compounds secreted from plant roots that can directly or indirectly affect plant growth and the microbial population of soils' [10]. Allelochemicals are a group of secondary metabolites produced by plants and microorganisms that promote plant growth [11]. However, when continuous cropping is practiced, allelochemicals build up in the soil. When the allelochemical content of soils exceeds a certain threshold, the germination, growth, survival and reproduction of neighbouring plants and microorganisms are suppressed [12]. These allelochemicals that have negative effects are referred to as auto-toxic compounds [11]. Numerous ACs have been extensively documented to serve as a unique carbon source for pathogenic bacteria [4]. Pathogenic bacteria become dominant, leading to an increase in the incidence of disease, which inhibits plant growth and decreases crop yield and quality [4]. Therefore, many researchers have used various materials to decrease AC concentrations, such as biochar [13–15].

Biochar is a carbon-rich solid product resulting from biomass pyrolysis under oxygen-limited conditions and at temperatures below 700 °C. Biochar has a large surface area [16]. Previous reports indicate that biochar, which is used as a soil amendment, contributes to the improvement of crop productivity through the addition of nutrients (including effective N, effective P and effective K) and hormone analogues of biochar surface compounds to mitigate continuous-cropping obstacles [2,17]. In addition, the microbial populations and physical and chemical properties of soils improve with biochar treatment, which indirectly promotes plant growth [18]. More importantly, during pyrolysis, large quantities of carboxyl, carbonyl and ketone groups form on the surfaces of the biochar. In addition, other types of functional groups and porous structures are present in the biochar, which endow it with a strong adsorption capacity for organic and inorganic pollutants, mitigating the adverse effects of auto-toxic compounds on plants [19]. In particular, biochar effectively mitigates the continuous-cropping obstacles of tobacco, yielding significant outcomes [14]. However, the underlying mechanism for inhibiting the incidence rate of disease and promoting plant growth remains unknown. Our previous study indicated that in continuously cropped soil, biochar regulates soil PPO activity to suppress pathogens and decrease the incidence of root rot [12]. For auto-toxic compounds, continuous-cropping obstacles in soil originate from the long-term accumulation of autotoxins, including ginsenosides and phenolic acids [20]. Based on the favourable characteristics of biochar in terms of adsorption and the similarity of auto-toxic compounds to other contaminants, it can be inferred that auto-toxic compounds can be adsorbed by biochar, decreasing the concentration of auto-toxic compounds in continuously cropped soils. It has been proposed that biochar can improve soil conditions and absorb auto-toxic compounds through its rich pore structure, alleviating continuous-cropping obstacles. To ensure the universality of the research, tobacco was used in our study because it is a significant model plant and a typical crop susceptible to severe continuous-cropping obstacles. Therefore, in this study, we investigated soil allelochemicals in tobacco fields over 3 years and examined the interactions between biochar and these allelochemicals using laboratory adsorption tests. In addition, molecular dynamics and quantum chemical analyses were performed to elucidate the adsorption mechanism of allelochemicals on biochar. The primary objectives of this study were (1) to quantify and compare the dynamics of allelochemicals under varying doses of biochar, (2) to accurately determine the mechanism by which allelochemicals bind to biochar to elucidate the theoretical maximum adsorption potential of biochar and (3) to provide precise biochar doses for alleviating continuous-cropping obstacles in tobacco cultivation. The links between biochar and auto-toxic compounds established in this study will help soil scientists use precise amounts of biochar to relieve continuous-cropping obstacles in tobacco planting.

2. Materials and methods

2.1. Preparation of biochar

The tobacco straw used in this study was obtained from the Rice Research Institute of Shenyang Agricultural University, China. According to previous studies conducted in our laboratory, biochar produced at 450 °C from a laboratory muffle furnace is suitable for improving continuously cropped soil [12]. In these studies, biochar was produced in a factory; hence, we recommend that biochar be produced at 400 °C, which corresponds to an actual temperature of ~450 °C according to the instructions of the carbonisation furnace manufacturer. In the biochar preparation process, the material was pyrolysed under oxygen-limited conditions at 400 °C. The heating rate was 5 °C/min, and the final temperature was maintained for 30 min. This was followed by water cooling to room temperature. The biochar was produced in the preparation workshop of the National biochar Institute of China.

2.2. Measurement of biochar and soil properties

The chemical composition and physical structure of the biochar and soil were analysed in our study. The biochar (or soil) pH and electrical conductivity were measured with a 1:20 biochar-to-water ratio (or soil-to-water ratio) using a Multiparameter equipment (S475-uMix, Mettler Toledo Company, Shanghai, China). Biochar and soil samples were digested in a microwave system (ETHOS A, Milestone, Italy) equipped with pressurised vessels. A digestion solution of 6 mL of 65 % HNO_3 and 2 mL of 30 % H_2O_2 was used in the digested system. The digestion and extraction ($W_{soil/biochar}$:W_{water} = 1:20) solutions were analysed using ICP–MS (Aurora m90, Bruker, Germany) to understand the total and available nutrient content. The nitrogen adsorption Brunauer–Emmett–Teller method (BET/BJH

Surface Area, Micro-meritics, TristarII3020, USA) was used to analyse the biochar surface area. The surface functional groups of the biochars were identified using an Fourier transform infrared spectrometer (Tensor 27, Bruker, Germany). The physical dimensions of the biochar samples were determined using a field emission scanning electron microscope (Regulus 8100, Hitachi Limited, Japan). The biochar and soil properties are listed in Table S.

2.3. Field experiments

Weining (Guizhou in China, 26°39′54″ N, 104°41′90″ E) has red soil and a sub-tropical monsoon climate suitable for tobacco planting. High-quality tobacco leaves are produced in this region. Therefore, Weining is one of the main regions for tobacco production in China. Due to limited land resources in this area, tobacco is often planted in the same soil, resulting to severe continuous-cropping obstacles. Soils with various durations of continuous cropping can be found in this region. Therefore, sites with 3 years of continuous cropping were selected for our experiments. The first cultivated tobacco and continuous cropping of soil non-biochar treatment were used as controls. The soil of different biochar treatments included the following: Control (CK), soil first planted with tobacco amended with non-biochar treatment; Lz3, continuous-cropping soil amended with non-biochar treatment; Lz3B1, continuous-cropping soil amended with 20 tons/hectare tobacco biochar treatment; Lz3B3, continuous-cropping soil amended with 40 tons/hectare tobacco biochar treatment; Lz3B5, continuous-cropping soil amended with 60 tons/hectare tobacco biochar treatment; and Lz3B7, continuous-cropping soil amended with 80 tons/hectare tobacco biochar treatment.

2.4. Auto-toxic compound analysis

After harvest, rhizosphere soil (100 mg) from different biochar treatments was re-suspended in pre-chilled 80 % methanol and 0.1 % formic acid by well vortexing. The samples were incubated on ice for 5 min and then centrifuged at 15000 rpm at 4 °C for 5 min. Some of the supernatant was diluted to a final concentration containing 60 % methanol using LC–MS grade water. The extraction solutions were subsequently transferred to a fresh Eppendorf tube with a 0.22-μm filter and were then centrifuged at 15000 g at 4 °C for 10 min. Finally, the filtrate was injected into the LC–MS/MS system (Orbitrap Q Exactive HF-X mass spectrometer, Thermo Fisher, United States) to analyse the auto-toxic substance composition of the soil. Every treatment had three repetitions. The extract of method was used as our study according to Xie et al., 2019 [21].

LC–MS/MS analyses were performed using a Vanquish UHPLC system (Thermo Fisher) coupled with an Orbitrap Q Exactive HF-X mass spectrometer (Thermo Fisher). Extraction solutions were injected onto a Hyperil Gold column (100 × 2.1 mm, 1.9 μm) using a 16-min linear gradient at a flow rate of 0.2 mL/min. The eluents for the positive polarity mode were eluent A (0.1 % FA in Water) and eluent B (Methanol). The eluents for the negative polarity mode were eluent A (5 mM ammonium acetate, pH 9.0) and eluent B (Methanol). The solvent gradient was set as follows: 2 % B, 1.5 min; 2%–100 % B, 12.0 min; 100 % B, 14.0 min; 100%–2% B, 14.1 min; and 2 % B, 16 min. The Q Exactive HF-X mass spectrometer was operated in the positive and negative polarity modes with a spray voltage of 3.2 kV, capillary temperature of 320 °C, sheath gas flow rate of 35 arb and aux gas flow rate of 10 arb. The above method of LC-MS/MS was referred to Wang et al., 2019 [22].

2.5. Pot experiment, sample collection and plant traits

Due to environmental factors such as temperature and humidity, the concentration of allelopathic substances in soil samples from the field exhibited significant fluctuations. Pot experiments were designed to accurately illustrate changes in the actual concentration while excluding environmental impacts. Pot soils from continuous cropping for 3 years were provided by the Bijie Tobacco Company of Guizhou Province. The experiment was conducted at Zunyi Normal College, Guizhou Province, China (27°13′15″ N, 106°17′22″ E). Tobacco biochar (under 400 °C) was obtained from Shenyang Agricultural University, National biochar Institute, Shenyang, China. The size of the pots used in this part of the experiment was 35 cm × 35 cm with 5 kg of soil. The soil used in the pot experiment had the following properties: pH 5.12, total carbon (TC) 3.2 %, total nitrogen (TN) 0.34 %, TC:TN (C:N) 9.42, available NH_4^+–N 2.55 mg/kg, NO_3^-–N 126.14 mg/kg, PO_4^{3-}–P 25.28 mg/kg, K 217.53 mg/kg, extractable S 0.04 %, Mg 0.26 %, Ca 0.32 % and Al 12.3 mg/g (see below for the methods for soil analysis). According to the local fertilisation practices in Weining, chemical fertiliser (N: 6.6 g, P_2O_5: 5.4 g and K_2O: 14.2 g for every pot) was applied in our pot experiment to provide nutrients for tobacco growth. In each pot, one tobacco plant was planted. The pots included 8 treatments: MCK, continuous-cropping soil with no biochar treatment; M1, biochar content of 4 g/kg in pots; M2, biochar content of 8 g/kg in pots; M3, biochar content of 12 g/kg in pots; M4, biochar content of 16 g/kg in pots; M5, biochar content of 20 g/kg in pots; M6, biochar content of 24 g/kg in pots; M7, biochar content of 28 g/kg in pots. Every treatment included three repetitions.

Once the tobacco seedlings reached suitable growth conditions, they were transplanted into pots. Each pot contained one seedling. Finally, the pot experimental system was transferred into a walk-in incubator (Bio-Chambers TPC-37, Bio-chambers, Inc., Canada) to eliminate interference from environmental factors, further ensuring the accuracy of the experimental data. The pots were cultured under a 12 h light (25 °C)/12 h dark (20 °C) photoperiod at approximately 400 $mmol/m^2 \cdot s^1$ and approximately 70 % humidity [23].

Sixty days after tobacco was transplanted, plant height, stem thickness, leaf area, root weight and root volume from all treatments were analysed to evaluate the effects of biochar. In contrast, rhizosphere soils were collected by removing tobacco plants. Representative soils were obtained by combining the same treatment samples from three pots [24]. The 3 g soil samples were placed into a 50-mL centrifuge tube with 25 mL 1 mol/L NaOH and shaken at 120 rpm in the dark at room temperature (25 °C ± 0.5 °C) [25]. The mixed solutions with biochar and soil were centrifuged at 3000 rpm for 10 min. The supernatants were used for PHA analysis following

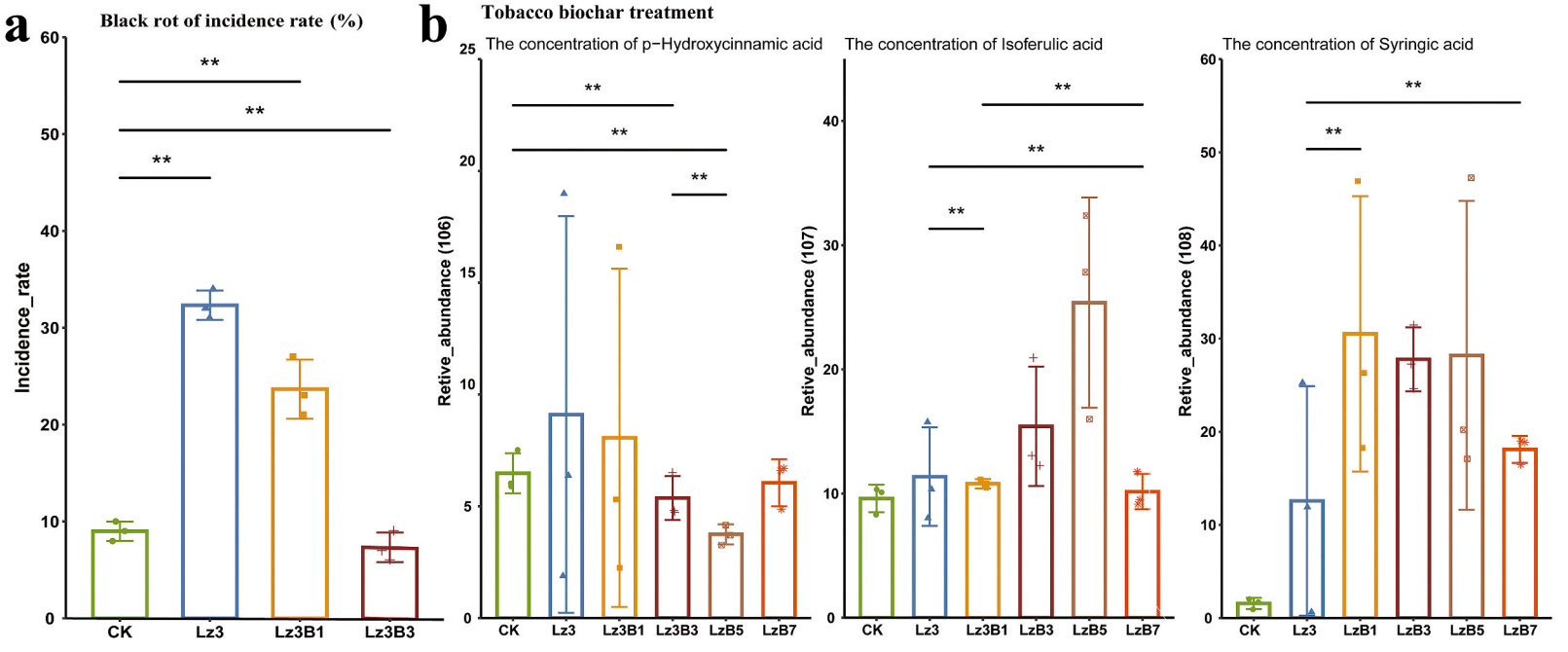

Fig. 1. (a) The black rot of incidence rate in continuous cropping tobacco field under non-biochar and tobacoo biochar treatment as follow: CK, soil first planting tobacco amended with non-biochar treatment; Lz3, continuous cropping soil amended with non-biochar treatment; Lz3B1 continuous cropping soil amended 20 tons/hectare tobacco biochar treatment; Lz3B3 continuous cropping soil amended 40 tons/hectare tobacco biochar treatment; Lz3B5, continuous cropping soil amended 60 tons/hectare tobacco biochar treatment; Lz3B7, continuous cropping soil amended 80 tons/hectare tobacco biochar treatment. (b) The concentration of *p*-Hydroxycinnamic acid, isoferulic acid and syringic acid under different biochar treated intensity from fields in Weining of Bijie city, Guizhou Province. The statistical significance based on Wilcoxon signed-rank test (two-sided, * means $p < 0.05$, ** means $p < 0.001$).

the above-mentioned protocol for UPLC–MS/MS.

Plant physiological characteristics were analysed to reflect the influence of biochar on tobacco. The Malondialdehyde (MDA) content was evaluated using the method of Meng et al. [26]. In brief, 100 mg of tobacco leaves were individually ground with liquid, and the homogenate was re-suspended in 1 ml of pre-chilled 10 % trichloroacetic acid. The sample was placed into 1.5-mL centrifuge tube and centrifuged at 8000×*g* for 10 min at 4 °C. Subsequently, 0.2 mL of the supernatant was placed into new 1.5-mL centrifuge tube with 0.6 ml of 0.6 % thiobarbituric acid. The mixture was heated at 95 °C for 30 min and quickly cooled in an ice bath. The cooled extracted solutions were centrifuged at 10000×*g* for 10 min at 4 °C. The supernatant absorbance was tested at 523 and 600 nm using a spectrophotometer (UH5700, Hitachi company, Japan). For Peroxidase (POD) and Superoxide Dismutase (SOD), 100 mg of leaves were ground and homogenised in an ice bath at a tissue mass (g):distilled water volume (mL) ratio of 1:10, 8000 × *g*, and centrifuged at 4 °C for 10 min, and the supernatant of POD and SOD contents were measured according to the reagent kit (Hongchen Biotechnology Co., Ltd., Shenyang, China) [27,28].

2.6. Disease index

Disease incidence (DI) was expressed as the percentage of diseased plants per total number of plants. Disease severity was investigated using fixed plants. Disease severity was scored on a scale of 0–4: 0 = no symptoms; 1 = less than half of the leaves on the diseased side were wilted, less than half of the stem circumference on the diseased spot or fewer lesions; 2 = half two-thirds of leaves on the diseased side of the stem circumference; 3 = more than two-thirds of leaves on the diseased side or completely susceptible to the stem by the disease spot; and 4 = all leaves were wilted or the plant was dead. The disease index was calculated using the formula described by Li [41]:

$$\text{Incidence rate} = \frac{N_D}{T} \tag{1}$$

$$\text{Disease index} = \frac{\sum_{i=1}^{4} \times N_i}{T}$$

where N_D is the number of diseased tobacco plants, T is the total number of tobacco plants surveyed, i is the scale of disease severity and Ni is the number of diseased tobacco plants at the corresponding disease severity.

2.7. Adsorption experiments

We analysed the concentrations of *p*-hydroxycinnamic acid (PHA), iso-ferulic acid (IA) and syringic acid (SA) under the different biochar treatment doses used in the fields in Weining, Bijie City, and found that the concentration of PHA decreased under biochar treatment, whereas the concentrations of IA and SA increased (Fig. 1b). Autotoxins are the root cause of continuous-cropping obstacles. In our experiment, the concentration of *p*-hydroxycinnamic acid was consistent with the incidence rate of black rot (Fig. 1a). Because of the porous structure of biochar, we expected that the *p*-hydroxybenzoic acid (PHA) concentration would be influenced by biochar treatment. We propose that the concentration of PHA decreases in response to adsorption by biochar. PHA from Invitrogen (Shanghai, China) was used in the absorption experiment. Adsorption experiments were conducted using a batch adsorption approach as described in previous studies. The absorption kinetics of PHA were tested using 100 mL vials sealed with plate covers. The 40 mL sorbate solution (50 mg/L PHA) was transferred to the vials, which contained 0.01 mol/L NaCl in ultra-pure water and 200 mg/L NaN_3 as a bio-inhibitor with stock solution. Subsequently, 0.05 g of biochar was dissolved in the sorbate solution. The solutions were at natural pH to report the absorption of BA on biochar. The vials were shaken at 120 rpm in the dark at room temperature (25 °C ± 0.5 °C). The PHA concentrations were investigated from 1 min to 25 h. The mixed solutions with biochar were centrifuged at 3000 rpm for 10 min. The equilibrium concentrations of PHA were analysed using UPLC–UV at a wavelength of 231 nm (ACQUITY UPLC I-Class-UV, Waters, USA). An AccQ-Tag Ultra-C18 Column (2.5 μm, 4.6 × 150 mm, 1/pk) was used to analyse the PHA concentration under biochar adsorption. Methanol with KH_2PO_4 (0.01 M, pH adjusted to 3.0 using phosphoric acid) (methanol-to-KH_2PO_4 ratio is 45:55) was used as the mobile phase with a 0.15 ml/min flow rate.

For the absorption isotherms of PHA, the equilibrium time and concentration were determined on the basis of kinetic experiments. Biochar (0.05 g) was added to a 50 mL stock solution. The initial concentration of PHA (0.5–2 g/L) was used to obtain the desired equilibrium concentration from biochar. During this period, the vials were agitated at 120 rpm in the dark at room temperature (25 °C ± 0.5 °C) for 24 h until adsorption equilibration. UPLC–UV was used to analyse the PHA concentration as mentioned above. All experimental data were obtained from the average values of three parallel samples. The details of the regression analysis for the kinetic and isotherm models are listed in Text S1. According to previous literature, UI software was used to fit the isothermal and kinetic models to the experimental data [2,29]. Origin 8.1 was used to draw the fitting curves for the isothermal and kinetic models.

2.8. DFT calculations

The biochar structure (under 400 °C preparation conditions) was determined from previous literature (173 atoms and a molecular weight of 1615 Dal). Because large molecular calculations are time-consuming, DFT was used in our experiment. The geometry optimisation of molecules, including biochar, biochar residuals and PHA, was computed using DFT with the B3LYP functional with the

6–311/G** basis set, and the DFT-D3 (BJ) dispersion correction was used with free movement from the whole system. The single energies of molecules were analysed at a level of M06-2X/6–311 + G (2d, p) to influence weak interactions.

The following formula was used to exhibit the interaction energy (E_i):

$$E_i = E_{(\text{biochar or biochar residuals+PHA})} - E_{(\text{biochar or biochar residuals})} - E_{(\text{PHA})}$$

where $E_{(\text{biochar or biochar residuals+BA})}$ reflects the total energy of biochar/biochar residuals + PHA, $E_{(\text{biochar or biochar residuals})}$ is the total energy of biochar/biochar residuals and $E_{(\text{PHA})}$ represents the total energy of PHA.

Gaussian 16 (A.03) software was used for all quantum chemistry calculations. The multi-wfn programme was used to analyse the electronic structure, localised molecular orbitals, quantitative molecular surface analysis and weak interactions according to the manual. The iso-surface maps of various orbitals and real space functions, exported from Multi-wfn files, were visualized using the visual molecular dynamics software.

2.9. Data and statistical analysis

The raw data files generated by UHPLC–MS/MS were processed using Compound Discoverer 3.0 (CD 3.0, Thermo Fisher) to perform peak alignment, peak picking and quantitation for each metabolite. The main parameters were set as follows: retention time tolerance, 0.2 min; actual mass tolerance, 5 ppm; signal intensity tolerance, 30 %; signal-to-noise ratio, 3; and minimum intensity, 100000. Next, peak intensities were normalised to the total spectral intensity. The normalised data were used to predict the molecular formula based on additive ions, molecular ion peaks and fragment ions. The peaks were matched with the mzCloud (https://www.mzcloud.org/) and ChemSpider (http://www.chemspider.com/) databases to obtain accurate qualitative and relative quantitative results. The data were analysed through the free online platform of majorbio choud platform (cloud.majorbio.com)[30].

One-way analysis of variance was used to analyse the difference in soil properties after biochar application using SPSS (V 23.0, IBM Corporation). Student's t-test (*t*-test) and Tukey's HSD were performed to examine soil properties and agronomic characteristics using R software.

3. Results

3.1. Effects of biochar on autotoxins from field experiments

To investigate the variation in the autotoxin concentration of soil with continuous-cropping obstacles under different biochar treatment intensities, the disease index and untargeted metabolomics of tobacco rhizosphere soil are shown in Tables S4 and S5. Soil samples were collected and representative of the main production region of tobacco grown for 3 years with a high black rot incidence rate (Fig. 1a). Furthermore, biochar addition significantly decreased the incidence rate of black rot in three continuous-cropping fields, in line with previous literature [13]. Biochar is beneficial for many plants, such as soybean, tobacco and watermelon, and it promotes plant growth and decreases DI in continuous cropping [31,32]. Many studies have indicated that processing is related to autotoxin concentrations. We hypothesised that autotoxin concentrations decrease in continuous-cropping soil. Next, we tested this hypothesis using untargeted compound analysis based on UPLC–MS/MS. The biochar treatment noticeably affected the concentrations of three autotoxins: PHA, IA and SA(Fig. 1b).

Most notably, the incidence rate of black rot slightly decreased from 34 % to 6 % ($p < 0.01$). The values peaked in Lz3B3 (6 %), which was much lower than those in CK (Fig. 1b). It was logical that biochar effectively inhibited the incidence of black rot. Simultaneously, the relative abundance of PHA sharply decreased from 9.10×10^6 to 6.48×10^6 under biochar treatment, which was less than that in Lz3 ($p < 0.01$), in contrast to IA and SA (Fig. 1b and Table S1, $p < 0.001$). In our study, the concentration of IA peaked in Lz3B5 (27.61×10^6 relative abundance) compared with that in Lz3B1 (29.71×10^6 relative abundance) under biochar treatment. Overall, the concentrations of the two autotoxins were far greater than that of Lz3 ($p < 0.01$). The accumulation of autotoxins is an obstacle to continuous cropping, consequently inhibiting plant growth and making plants vulnerable to diseases and insect pests. The trend is linear in the PHA concentration change under biochar treatment. Therefore, decreasing autotoxin concentration was correlated with the biochar treatment of soils [4]. Overall, it is highly probable that biochar relieves the continuous-cropping obstacles of tobacco by weakening the PHA concentration in the soil in tobacco fields. Based on this point, further studies should focus on the interactions between biochar and PHA. Notably, the standard deviation values strongly fluctuated (Fig. 1b). This result may be related to the complex environment in the field. To avoid environmental influence, a pot experiment was performed to eliminate interference from a complex environment to effectively reduce autotoxin fluctuations.

3.2. Biochar decreases the PHA concentration and remaining tobacco qualities in pot experiments

To further investigate the influence of biochar on alleviating the continuous cropping of tobacco, a pot experiment was used to eliminate the effect of environmental factors, including rainfall and temperature. In our experiment, the leaf area (from 2705.45 ± 264.84 to 3266.13 ± 356.37 mm^2) gradually increased in the initial stage of biochar treatment (Fig. S2) under M1–M8 and decreased in M7. Comparing plant height, the trend gradually decreased from M1 to M7. Leaf area is crucial for tobacco production. An increase in leaf area may cause stem lodging. Therefore, many agronomists have shown that reducing plant height can effectively reduce plant lodging. In our study, biochar promoted an increase in leaf area and a decrease in plant height, which is beneficial for tobacco

production. However, whether the quality of tobacco is influenced by increasing leaf area has not been reported. Therefore, we tested the nicotine, Cl and K contents, which affect the quality of tobacco. Nicotine is an important indicator of tobacco quality. The total amount of nicotine showed a significant increasing trend with increasing biochar treatment intensity. The nicotine content of M7 (1.46 %) was higher than that of the other biochar treatments, increasing by 167.46 % compared with that of MCK (non-biochar, 0.55 % nicotine, $p < 0.05$, Table S2). In contrast, tobacco is a Cl-free plant. Cl is essential for tobacco growth. In the biochar treatment, the Cl level in tobacco leaves was significantly lower than that in MCK (0.25 %, $p < 0.01$), with a trend towards first decreasing and then increasing (from 0.11 % to 0.23 %). In contrast, the K content in tobacco leaves first increased and then decreased with biochar treatment intensity, which was consistent with the sugar and protein contents. The trend of K in the biochar treatment was M2 > M3 > M4 > M5 > M6 > M7 > M1 > MCK (increasing from 31.75 % to 128.57 %). The overall results indicated that biochar application affected the reduction of sugar, protein, Cl and K contents in tobacco plants.

To further examine the underlying mechanisms, we correlated the distance-corrected dissimilarities of agronomic traits and physiology with soil factors (Fig. 2a). Overall, the agronomic traits of tobacco plants had the strongest correlations of organic matter (OM), pH, total phosphorus (TP), total potassium (TK), TN, available potassium (AK) and available phosphorus (AP), while a significant correlation of physiology was found for AN, AP and AK. In contrast, the theory of free radicals suggests that damage due to reactive oxygen species is one of the causes of plant leaf senescence. Under normal circumstances, the free radical scavenging system in the plant body can effectively prevent damage caused by reactive oxygen species and reduce the MDA content and accumulation of O^{2-} and H_2O_2 in cells. With increasing MDA, SOD and POD, the degree of membrane lipid peroxidation intensifies, thereby accelerating the ageing process of tobacco plants. In our study, except for AN, the POD of tobacco was negatively correlated with soil factors compared with that of reducing sugar, which was correlated with AN ($R^2 = 0.53$, $p < 0.01$). MDA and SOD were not affected by soil factors. The results indicated that soil factors decreased tobacco plant senescence. In addition, soil variables other than AN enhanced leaf area. Furthermore, the Cl and nicotine content of plants increased appropriately under soil factors.

All factors improving continuous-cropping soil originated from the biochar treatment intensity (Fig. 2d). We observed that the OM ($R^2 = 0.97$, $p < 0.001$), pH ($R^2 = 0.91$, $p < 0.001$), AK ($R^2 = 0.83$, $p < 0.001$), TP ($R^2 = 0.98$, $p < 0.001$), AP ($R^2 = 0.91$, $p < 0.001$), TK ($R^2 = 0.89$, $p < 0.001$) and TN ($R^2 = 0.53$, $p < 0.008$) of the soil strongly correlated with the biochar treatment intensity. Furthermore, the PHA and SA of continuous-cropping soil significantly decreased with increasing biochar intensity ($p < 0.01$). There was no obvious difference in IA. Therefore, black rot was not observed in the pot experiment.

Tobacco growth is affected by nutrient, light and temperature conditions. Overall, biochar decreased the autotoxin concentration and provided a low-toxicity environment for tobacco growth (Fig. 1b). With biochar application, SOD, POD and MDA were regulated to reduce the accumulation of O^{2-} and H_2O_2 (Fig. 2c). Residual nutrients in biochar are rich sources of mineral elements for tobacco growth. The results suggested that biochar directly affected soil factors, indirectly improved individual leaf area and inhibited plant ageing. Meanwhile, the quality of tobacco remained unchanged.

In the pot experiment, the trend of the PHA concentration in the biochar treatment was linear in the field. The PHA concentration decreased in the different biochar treatments (Fig. 2b). We considered that biochar can alleviate continuous cropping by decreasing PHA concentrations. In previous reports, because of its rich pore and surface area, biochar has been used as a soil amendment to decrease pollutant concentrations. We considered that PHA was adsorbed on biochar, which decreased its concentration. We designed an experiment to demonstrate PHA adsorption on biochar to support this hypothesis.

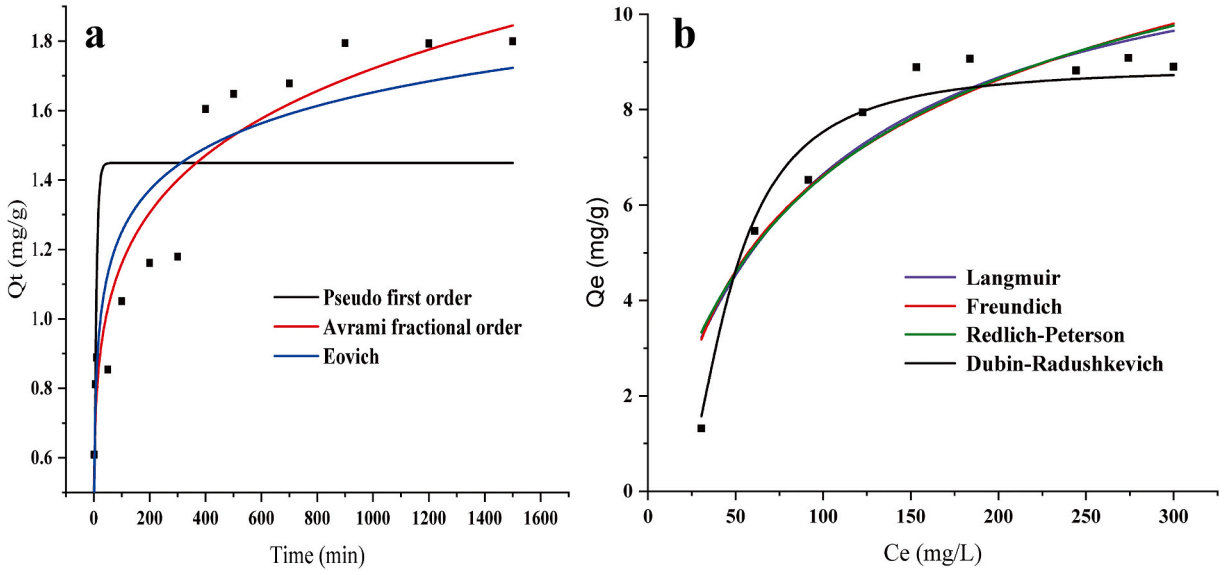

Fig. 2. (a) Kinetic fitting results of *p*-Hydroxycinnamic acid removal by biochar, C_0 = mg/L, pH = 8.3, m/V = 0.5 g/L, and T = 25 °C. (b) Isotherm fitting results of *p*-Hydroxycinnamic acid absorbed on biochar, C_0 = 0.5–15 mg/L, pH = 8.3, m/V = 0.5 g/L, and T = 25 °C, $t_{adsorption}$ = 350 min.

3.3. Adsorption of PHA on biochar

Kinetic adsorption models, including Pseudo_first_order, Pseudo_second_order, Avrami fractional order, Elovich and Intra_particle diffusion equations, have been widely used to analyse the influence of contact time between adsorbate and adsorbent. The fitting results are shown in Fig. 3a. The initial sorption rate of PHA on the biochar was fast. There was almost an adsorption equilibrium within 450 min (approximately 88.3 % PHA). Then, with increasing time, the rate of sorption became flat. However, there was no endpoint to indicate the equilibrium between BA and biochar within approximately 1000 min. Therefore, PHA adsorption on biochar was considered to be a slow process.

The parameters of the kinetic models are presented in Table 1. The Pseudo_first_order had a higher correlation coefficient (R^2 = 0.9297) than the Avrami_fractional_order model (R^2 = 0.8363) and the Eovich model (R^2 = 0.9234). The results suggested that the sorption process between PHA and biochar can be classified as physical sorption, which reached a reversible equilibrium. Furthermore, the Eovich model was excellently fitted to our data. The model was used to describe the predominant chemisorption on highly heterogeneous sorbents. Therefore, the chemical interaction between the active site of the biochar surface and the PHA in solution was considered in our experiment.

For the sorption isotherms, biochars were affected by the raw material and temperature. The physico-chemical properties of biochars were different from each other due to structural changes and the loss of volatile organics. The Langmuir, Freundlich, Temkin, Sips, Redlich–Peterson and Dubinin−Radushkevich models were used in our experiment to analyse the mechanism of biochar absorption. The sorption isotherms of PHA on biochar are presented in Fig. 3b, and the related parameters are listed in Table 2. The results indicated that the Langmuir, Freundlich, Redlich–Peterson and Dubinin–Radushkevich models were suitable for our data (R^2 > 0.5). However, the data were not fitted by the Temkin and Sips models. The theory of the Langmuir model considers that monolayer sorption mainly occurs at specific homogeneous sites, whereas the Freundlich model assumes that a heterogeneous surface is the main factor. Nevertheless, the two models were restricted by the absorbent concentration. Therefore, the Redlich–Peterson model, which is widely used as a compromise between the Langmuir and Freundlich models, was used to approximate the adsorption data to address the absorbent concentration. The β_{RP} included in the Redlich–Peterson model was an exponential factor ranging from 0 to 1. When β_{RP} = 0 became the Langmuir model, β_{RP} = 1 became the Freundlich model. In our experiment, the Freundlich model had better parameters (R^2 = 0.9986) than the Langmuir model (R^2 = 0.8821). The results suggested that the biochar presented variable types of adsorption sites. In other words, multi-layer adsorption on non-uniform surfaces played an important role in the absorption mechanism of biochar. Moreover, the Redlich–Peterson model of three parameters was the best fitted to the Langmuir and Freundlich models (R^2 = 0.9997). This indicates the potential coexistence of heterogeneous and monolayer sorption. However, β_{RP} (0.9113), which was close to 1, indicated that heterogeneous adsorption played a more important role than monolayer adsorption in the BA and biochar interaction. In contrast, the biochar maximum sorption capacity of PHA was 12.4831 mg/g. Therefore, in theory, biochar can effectively reduce the content of self-toxic substances (PHA) through heterogeneous adsorption. For the field performance of biochar

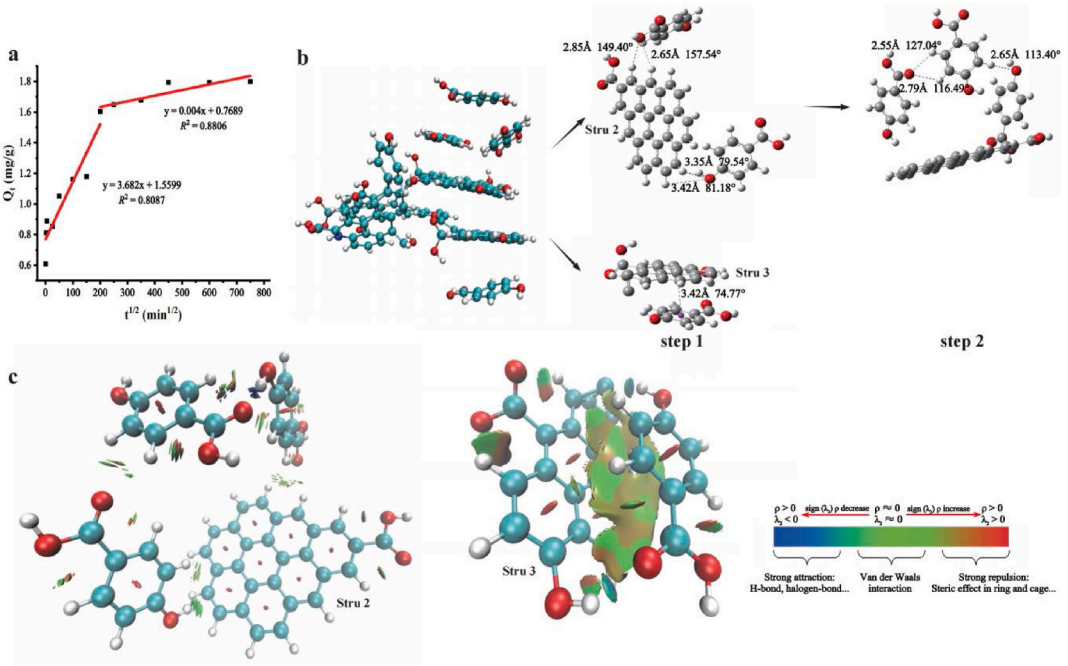

Fig. 3. (a) Intraparticle diffusion plot for *p*-Hydroxycinnamic acid adsorbed on biochar, C_0 = 0.5–15 mg/L, pH = 8.3, m/V = 0.5 g/L, and T = 25 °C, $t_{adsorption}$ = 350 min. (b) MD and DFT analysis basing on GROMACS and GAUSSINON 16. (c) non-covalent interactions between *p*-Hydroxycinnamic acid and biochar by the IGM showing the visualized weak interaction region.

Table 1
The fitting results of PHA on biochar using Pseudo first order, Avrami fractional order and Eovich models.

Pseudo_first_order model		Avrami_fractional_order model		Eovich model	
qe (mg/g)	8.0758	qe (mg/g)	6.8998	qe (mg/g)	8.4739
k1 (min-1)	0.004	*k2 (g mg-1min-1)*	0.0552	*kAV (min-1)*	0.0037
R2	0.9297	*R2*	0.8363	N	0.7687
				R2	0.9234

Table 2
Isotherm parameters of Langmuir (L), Freundlich (F), Redlich_Peterson (RP), Dubin-Radushkevich (DR) from fitting PHA adsorption on biochar.

Temp	Model	parameter 1	parameter 2	parameter 3	R2
25 °C	L	qmax = 12.4831 mg/g	KL = 0.0114 L/mg		0.8821
	F	KF = 2.8985 (mg/g)(L/mg)1/n	nF = 0.0981		0.9986
	RP	KRP = 0.1639 (L/g)	αRP = 0.0223 (L/mg)1/βRP	βRP = 0.9113	0.9997
	DR	QDR = 8.8892 mg/g	E = 2.4598 kJ/mol		0.8753

for PHA adsorption, further field tests are required.

The Dubinin–Radushkevich model has been used to distinguish between physical and chemical sorption. In our experiment, the fit of the model was 0.8753 (R^2). Therefore, the model was used to analyse the PHA of biochar sorption, which is a physical or chemical process. The *E* value of PHA was calculated as 2.4598 kJ/mol using the Dubinin–Radushkevich equation, which was lower than 8 kJ/mol. The results showed that physical sorption played a more important role than chemical sorption. Therefore, the interactions between biochar and PHA may depend on hydrogen bonding, π-interactions or hydrophobic interactions instead of chemical reactions with functional groups.

3.4. Mechanism of biochar to remove PHA on theory

To understand the biochar–PHA H-bond better, we used the MD method to observe the trajectories of interactions between biochar and PHA (Fig. 4b) to better understand the adsorption. In this study, four PHA molecules were absorbed by biochar. The process of absorption includes two steps. Structure 2 of the biochar first absorbed 2 PHA molecules, and Structure 3 of the biochar first absorbed 1 PHA molecule. Then, Structure 2 of the biochar absorbed one PHA molecule again. The results were excellent in explaining the two stages of biochar adsorption kinetics on PHA (Fig. 4a), including a steep adsorption capacity in the first step and a relatively flat adsorption capacity in the second step. To prove the reliability of the conclusion, 2 steps were calculated using the DFT method for Structure 1. MD and DFT results are consistent. For the DFT calculations, two PHAs formed two H-bonds with biochar in the first step. However, the strength of the H-bond between the two molecules and biochar was different, including one moderate (2.65 Å, 157.51° and 2.85 Å, 149.40°) and one weak (3.35 Å, 79.54° and 3.42 Å, 81.18°). In the second step, 1 PHA interacted with the previously absorbed 2 PHA on biochar via 3 H-bonds (2.55 Å, 127.04°; 2.65 Å, 113.40°; and 2.79 Å, 116.49°). H-bonds were mainly formed between carboxyl oxygen and hydrogen on the benzene ring. For Structure 3 of biochar, π–π interactions (3.42 Å, 74.77°) were suggested to be one of the most important adsorption mechanisms for biochar and PHA. Therefore, from the MD and DFT results, the biochar could theoretically adsorb 4 PHAs.

Observing weak interactions using a visual study between the absorbate and adsorbent is an extremely novel method for exploring adsorption mechanisms. In contrast, the Multi-wfn software is an excellent tool for the visual study of weak interactions. Therefore, IGM molecular surface analyses based on pro-molecular density were conducted to reveal other non-interaction analyses using Multi-wfn software. The blue–green–red colour transition of the iso-surface was used to distinguish the interaction region through the colour change. In this study, there were more green peaks and several blue peaks in Structure 2 of the biochar (Fig. 4c). The green region of the iso-surface indicates more vdW interactions. The blue region refers to the H-bond. Therefore, the IGM iso-surface displays weak interaction regions, and the double-bond oxygen in the carboxyl group from PHA could form vdW interactions with hydrogen atoms on the benzene ring of Structure 2 of the biochar or PHA. Meanwhile, the H-bond between the double-bond oxygen in the carboxyl group and the hydroxyl O atom of PHA is presented in the blue region. For Structure 3 of the biochar, the steric effect and vdW between the ring of PHA and the ring of Structure 3 are presented in the green and brown regions. This region may be the strong π–π bond.

In summary, the vdW, π–π bonds and H-bonds between the biochar and PHAs are the dominant factors that affect the adsorption capacity from MD, DFT and IGM analyses. In this section, we accurately calculated the adsorption ratio and mechanisms between biochar and PHA from theory in an autotoxin study in contrast to previous literature based on adsorption kinetics and thermodynamic analysis. The accurate results indicated that $N_{biochar}$:N_{PHAs} was equal to 1:4. Based on the MD theory, the process for the adsorption of PHA on biochar is shown in Movie S.

4. Discussion

Our results from experiment and theory analysis proved our hypothesis. Biochar can decreased autotoxin concentrations though absorption in order to continuous cropping of tobacco. van der Waals force (vdW), π-π bonds and H-bonds played an important role in

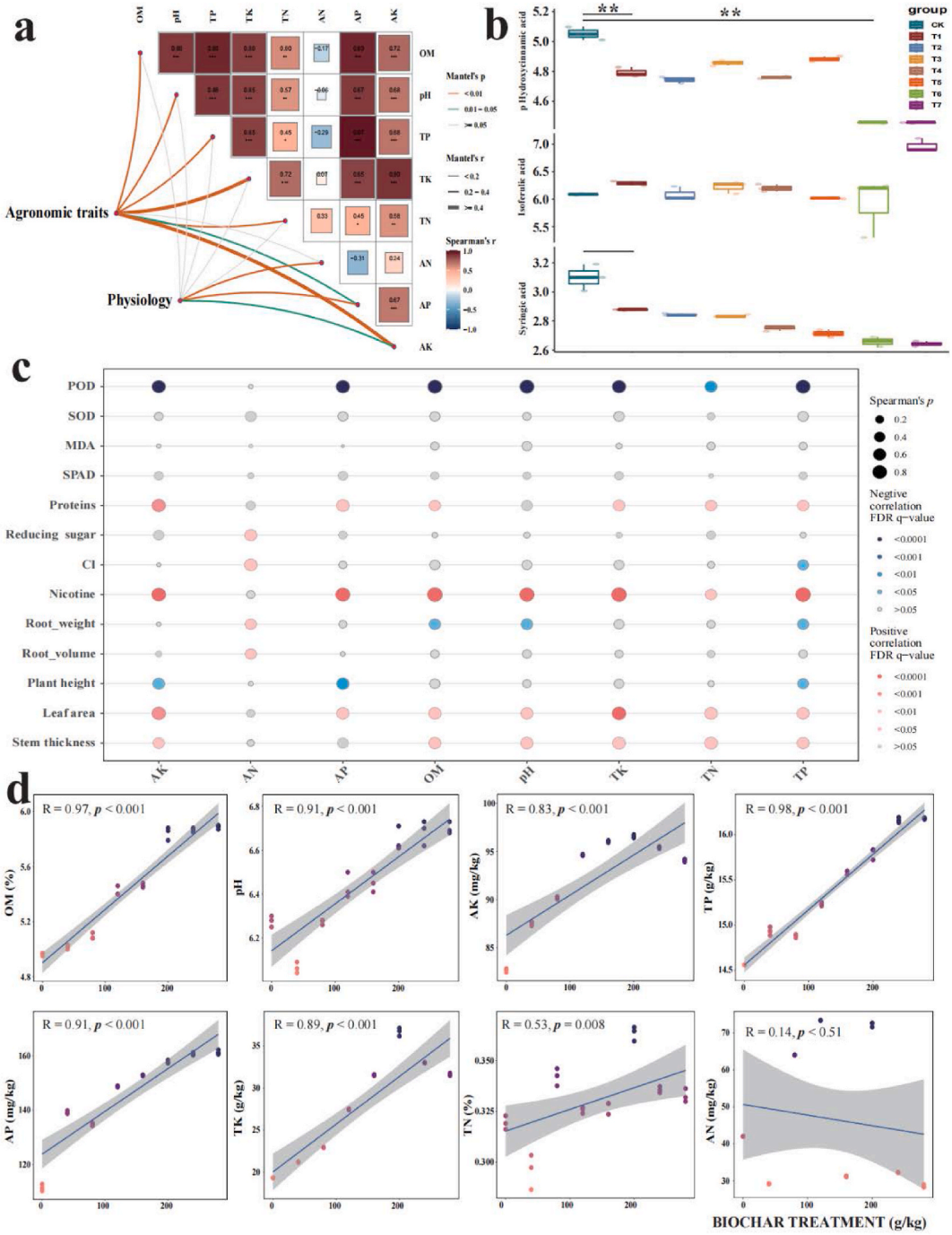

Fig. 4. (a) Pairwise comparisons of soil factors are showed, with a color gradient denoting Spearman's correlation coefficient. Agronomic traits and physiology of tobacco was related to each soil factor by Mantel test. Line width is related to the Mantel's *r* statistic for the corresponding distance correlations, and the line color contributed to the statistical significance. (b) The concentration of *p*-Hydroxycinnamic acid, isoferulic acid and syringic acid in different biochar treatment with Wilcoxon signed-rank test (two-sided, * means $p < 0.05$, ** means $p < 0.001$). (c) The spearman correlation of soil factor with agronomic traits and physiology of tobacco. The bubble color gradient represented the adjusted *p*-values levels (the red denoted positive correlation and the blue denoted the negative correlation). The bubble size denoted the correlation levels. (d) Correlations between the soil factor and biochar treatment intensity.

absorption PHA on biochar.

Soil microorganisms play an important role in soil processes, including the nutrient cycle, organic compound turnover and toxin degradation. The microbial community is influenced by environmental changes [33]. When biochar is used as a soil amendment, the

soil microbial community undergoes changes. Therefore, studies on the interactions among biochar, autotoxins and rhizosphere microorganisms could lay a theoretical foundation for alleviating obstacles to continuous cropping. In our previous experiments, we demonstrated that biochar regulates soil PPO activity in continuously cropped soil to suppress pathogens and decrease the incidence of root rot [12]. This conclusion aligns well with reports from previous literature [17]. However, the relationship between biochar and autotoxins in tobacco fields has not yet been determined. Rhizosphere microorganisms were not included in our study. Instead, we focused on the relationship between biochar and autotoxins.

Biochar is an excellent material for adsorption due to its large surface area and is used to decrease organic and inorganic pollution [34]. Autotoxins are the main factors that increase plant vulnerability to diseases. Autotoxins present in plant rhizospheres may be considered organic pollutants that affect plant growth. Based on this viewpoint, the autotoxin concentration could be decreased by biochar absorption, thereby reducing DI. In our experiment, the incidence of black rot in continuously cropped soil decreased with increasing biochar dose. Wang et al. and Ma et al. reported that the concentration of autotoxins in soils is reduced by the addition of biochar and that tobacco growth is promoted [29,35] Therefore, biochar treatment could influence the autotoxin concentration to reduce the DI rate [36]. β-cembrenediol, din-butyl phthalate, diisobutyl phthalate, ferulic acid, benzoic acid, phthalates and phenolic acids are considered essential autotoxins in tobacco [20]. In our study, PHA was determined to be an auto-toxic compound that affected the black rot incidence rate. In addition, the PHA concentration was influenced by the biochar dose. PHA is considered as an important auto-toxic compound according to previous literature [37]. biochar could decrease soil PHA concentration through absorption to relieve the obstacles associated with the continuous cropping of tobacco plants. Many studies have focused on biochar to change the soil micro-flora and alleviate continuous-cropping obstacles [2,38]. There are several reports on the interaction between autotoxins and biochar. Our adsorption experiment proved that biochar could absorb PHA. DFT and molecular dynamics analysis also confirmed these findings. Evidence of adsorption between biochar and PHA supports our previous hypothesis from experiment and theory. On the other hand, Autotoxins cause continuous-cropping obstacles in soil [4]. To date, an accurate dosage of biochar for alleviating continuous cropping of soil has remained unknown. In our experiment, we considered the accurate dosage of biochar to be 8 g/kg (M2), which is the best dosage for continuous cropping, based on pot, adsorption experiments, DFT and molecular dynamics analysis.

Biochar is the best approach for promoting plant growth [39]. Bio-functional organic compounds from biochar can promote crop-stress resistance [40,41], nitrogen-use efficiency [42] and plant growth [43]. However, the influence of organic compounds is only 21 days [43]. Therefore, we do not believe that continuous-cropping obstacles can be alleviated by organic compounds from biochar. In our experiment, we found that biochar may alter the physical and chemical properties of soil, such as OM and pH. The pore structure and surface functional groups of biochar carry residual nutrients, regulate acidity and alkalinity and increase the conductivity of soils [19]. Biochar decreased nutrient leaching losses. Therefore, the nutrient content of the biochar-treated soil was greater than that of the un-amended soil in our experiment (Fig. 2d). The nutrient levels of soils affect the agronomic traits of crops, including leaf area and stem thickness. The strongest relationships observed existed between nutrients and agronomic traits (Fig. 2a–c). Ren et al. reported that the agronomic traits and physiology of tobacco plants are influenced by soil properties [44]. In addition, a pH of 5.6–7 is suitable for ensuring tobacco growth. The biochar pH was >7.0. Biochar can neutralise acidity in soils [19]. Biochar amendment results in a suitable pH for tobacco growth under different biochar treatments (pH 5.8–6.5). Nicotine concentration is an important indicator of tobacco plant quality. Tobacco quality indicators, such as nicotine concentration, are affected by the addition of biochar. These results are in alignment with reports in previous literature [44,45]. Biochar can increase nicotine concentration, which improves the quality of tobacco plants. Our findings differ from those of studies using the microbial profile or autotoxins, which affect plant growth [44]. Our results indicate that biochar alleviates the toxicity of autotoxins from continuous-cropping soil, promoting tobacco growth by altering soil properties.

In our experiment, DFT and the IGM molecular surface were used to analyse the interaction between biochar and PHA. Visualisation clarified the adsorption site and processing of PHA on biochar. We accurately calculated that vdW, π–π bonds and H-bonds between the biochar and PHA were the dominant bonds, and a biochar molecule could absorb four molecules of PHA. The results are found in pollutant adsorption on biochar [46,47]. DFT, IGM and molecular dynamics were the first to be used to study autotoxin adsorption on biochar.

To relieve continuous-cropping obstacles in tobacco fields, management focuses on the application of chemical agents to kill soil-borne pathogens. However, their excessive utilisation results in hazardous environmental risks. Furthermore, there are high concentrations of auto-toxic compounds in the soil. Chemical agents cannot eliminate the influence of continuous cropping of soil. Therefore, methods for breeding superior varieties and inducing plant resistance are needed to overcome continuous-cropping obstacles. However, the two methods require more time for breeding. At present, most tobacco planting areas grow monotonous varieties. biochar is an environmentally friendly material. In our experiment, the application of biochar in continuous-cropping soil effectively decreased the concentration of autotoxins, inhibited the incidence of black rot and promoted tobacco growth. Therefore, biochar is an essential material for relieving continuous-cropping obstacles in sustainable agriculture.

The sample of soil from our study located at high altitude region for producing high-quality tobacco leaves (average altitude: 3000–4000 m). The solution is to alleviate the obstacles to continuous cropping of tobacco. In our previous study, biochar can alleviate tobacco continuous cropping. So, we exploded mechanisms. Therefore, the prevention and mitigation of obstacles to continuous tobacco cultivation in high-altitude environments for producing high-quality tobacco have certain production guidance significance.

5. Conclusion

The addition of biochar significantly inhibited the incidence of black rot and PHA concentration in both pot and field experiments.

However, SA and IA were enhanced with increasing biochar intensity, which is contrary to the allelochemical accumulation results in continuous-cropping obstacles. Therefore, further adsorption of PHA onto the biochar was conducted. The results indicated that the interactions between biochar and PHA mainly originated from the monolayer sorption process based on kinetic and isotherm adsorption models. We accurately calculated that vdW, π–π bonds and H-bonds between biochar and PHA are the dominant binding interactions from MD, DFT and IGM analyses. More importantly, we determined that a biochar molecule could absorb four molecules of PHA. Finally, the correlation of biochar intensity, soil properties, agronomic traits and bio-chemical indicators indicated that biochar effectively decreased the auto-toxicity effect in continuous-cropping soil. Furthermore, biochar markedly enhanced nutrient retention, further promoting tobacco growth.

Funding

This study received funding from the S&D Program from Bijie Tobacco Company of Guizhou Province (2021520500240048, 2018520500240066, 2023XM15), Characteristic Field Project in Guizhou Provincial Department of Education (KY[2020]058), Academic New Seedling Cultivation and Innovation Exploration Project (XM[2021]1–3), Special project of rural revitalization form Guizhou Provincial Department of Education (KY[2012]017-1), Zunyi Normal University Service Local Industrial Revolution Project (CXY[2021]03), National Guide to Guizhou Provincial Project (QKHZYD[2023]019).

CRediT authorship contribution statement

Haijun Hu: Methodology, Funding acquisition, Formal analysis, Data curation, wenfu chen, Writing – review & editing. **Jun Meng:** Software, Resources. **Huan Zheng:** Formal analysis, Data curation. **Heqing Cai:** Visualization, Validation, Supervision, Software, Project administration. **Maoxian Wang:** Writing – review & editing, Writing – original draft. **Zhenbao Luo:** Supervision, Software, Resources, Project administration, Conceptualization. **Yang E:** Writing – review & editing, Software, Methodology, Funding acquisition. **Caibin Li:** Funding acquisition. **Qiaoxue Wu:** Resources, Project administration, Methodology, Investigation. **Zhiqiang Yan:** Methodology, Investigation, Formal analysis. **Yue Lei:** Visualization, Validation.

Declaration of competing interest

The authors declare the following financial interests/personal relationships which may be considered as potential competing interests: YANG E reports financial support was provided by Shenyang Agricultural University. Yang E reports a relationship with Shenyang Agricultural University that includes: employment. If there are other authors, they declare that they have no known competing financial interests or personal relationships that could have appeared to influence the work reported in this paper.

Appendix A. Supplementary data

Supplementary data to this article can be found online at https://doi.org/10.1016/j.heliyon.2024.e33011.

References

[1] Y.D. Chen, J.F. Du, Y. Li, H. Tang, Z.Y. Yin, L. Yang, X.H. Ding, Evolutions, managements of soil microbial community structure drove by continuous cropping, Front. Microbiol. 13 (2022) e839494, https://doi.org/10.3389/fmicb.2022.839494.
[2] N. Zhou, C.M. Mei, X.Y. Zhu, J.J. Zhao, M.G. Ma, W.D. Li, Research progress of rhizosphere microorganisms in Fritillaria L. medicinal plants, Front. Bioeng. Biotechnol. 10 (2022) e1054757, https://doi.org/10.3389/fbioe.2022.1054757.
[3] W.S. Shen, M.C. Hu, D. Qian, H.W. Xue, N. Gao, X.G. Lin, Microbial deterioration and restoration in greenhouse-based intensive vegetable production systems, Plant Soil 463 (2021) 1–18, https://doi.org/10.1007/s11104-021-04933-w.
[4] Y.D. Chen, L. Yang, L.M. Zhang, J.R. Li, Y.L. Zheng, W.W. Yang, L.L. Deng, Q. Gao, Q.L. Mi, X.M. Li, W.L. Zeng, X.H. Ding, H.Y. Xiang, Autotoxins in continuous tobacco cropping soils and their management, Front. Plant Sci. 14 (2023) e1106033, https://doi.org/10.3389/fpls.2023.1106033.
[5] F.L. Wang, X.X. Wang, N.N. Song, Biochar and vermicompost improve the soil properties and the yield and quality of cucumber (Cucumis sativus L.) grown in plastic shed soil continuously cropped for different years, Agric. Ecosyst. Environ. 315 (2021) e107425, https://doi.org/10.1016/j.agee.2021.107425.
[6] M.J. Kwak, H.G. Kong, K. Choi, S.K. Kwon, J.Y. Song, J. Lee, P.A. Lee, S.Y. Choi, M. Seo, H.J. Lee, E.J. Jung, H. Park, N. Roy, H. Kim, M.M. Lee, E.M. Rubin, S. W. Lee, J.F. Kim, Rhizosphere microbiome structure alters to enable wilt resistance in tomato, Nat. Biotechnol. 36 (11) (2018) 1117–1126, https://doi.org/10.1038/nbt1118-1117.
[7] X.Y. Wang, Study on continuous cropping obstacle and control strategy of medicinal plants, Adv Soc Sci Educ Hum 119 (2017) 839–842.
[8] Z. Kai, G. Lanping, Z. Xiaobo, W. Chengxiao, Q. Yuan, L. Wei, Z. Tao, Z. Yayu, Y. Ye, Research progress on pesticide residues of Panax notoginseng, Zhongguo Zhongyao Zazhi 47 (6) (2022) 1438–1444, https://doi.org/10.19540/j.cnki.cjcmm.20211221.101.
[9] Y.L. Ku, W.Q. Li, X.L. Mei, X.N. Yang, C.L. Cao, H.M. Zhang, L. Cao, M.L. Li, Biological control of melon continuous cropping obstacles: weakening the negative effects of the vicious cycle in continuous cropping soil, Microbiol. Spectr. 10 (6) (2022), https://doi.org/10.1128/spectrum.01776-22.
[10] S. Latif, G. Chiapusio, L.A. Weston, Allelopathy and the role of allelochemicals in plant defence, Adv. Bot. Res. 82 (2017) 19–54, https://doi.org/10.1016/bs.abr.2016.12.001.
[11] J.R. Teasdale, C.P. Rice, G.M. Cai, R.W. Mangum, Expression of allelopathy in the soil environment: soil concentration and activity of benzoxazinoid compounds released by rye cover crop residue, Plant Ecol. 213 (12) (2012) 1893–1905, https://doi.org/10.1007/s11258-012-0057-x.
[12] S.H. Ge, J. Gao, D. Chang, T. He, H. Cai, M. Wang, C. Li, Z. Luo, Y. E, J. Meng, M. Gao, Biochar contributes to resistance against root rot disease by stimulating soil polyphenol oxidase, Biochar 5 (1) (2023), https://doi.org/10.1007/s42773-023-00257-3.

[13] D. Wu, W.M. Zhang, L.Q. Xiu, Y.Y. Sun, W.Q. Gu, Y.N. Wang, H.G. Zhang, W.F. Chen, Soybean yield response of biochar-regulated soil properties and root growth strategy, Agronomy 12 (6) (2022), https://doi.org/10.3390/agronomy12061412.

[14] D. Chen, M. Wang, G. Wang, Y.J. Zhou, X.E. Yang, J.Z. Li, C.P. Zhang, K. Dai, Functional organic fertilizers can alleviate tobacco (*Nicotiana tabacum L.*) continuous cropping obstacle via ameliorating soil physicochemical properties and bacterial community structure, Front. Bioeng. Biotechnol. 10 (2022) e1023693, https://doi.org/10.3389/fbioe.2022.1023693.

[15] X.X. Dong, Z.Y. Zhang, S.M. Wang, Z.H. Shen, X.J. Cheng, X.H. Lv, X.Z. Pu, Soil properties, root morphology and physiological responses to cotton stalk biochar addition in two continuous cropping cotton field soils from Xinjiang, China, PeerJ 10 (2022) e12928, https://doi.org/10.7717/peerj.12928.

[16] P. Wu, Z.Y. Wang, N.S. Bolan, H.L. Wang, Y.J. Wang, W.F. Chen, Visualizing the development trend and research frontiers of biochar in 2020: a scientometric perspective, Biochar 3 (4) (2021) 419–436, https://doi.org/10.1007/s42773-021-00120-3.

[17] X. Zhao, E. Elcin, L. He, M. Vithanage, X. Zhang, J. Wang, S. Wang, Y. Deng, N.K. Niazi, S.M. Shaheen, H. Wang, Z. Wang, Using biochar for the treatment of continuous cropping obstacle of herbal remedies: a review, Appl. Soil Ecol. 193 (2024) e105127, https://doi.org/10.1016/j.apsoil.2023.105127.

[18] A.G. Achakzai, S. Gul, A.H. Buriro, H. Khan, A. Mushtaq, A. Bano, S. Agha, K. Kamran, Z. Ponya, T. Ismail biochar-fertilizer mixture: does plant life history trait determine fertilizer application rate? Env Pollut Bioavail 35 (1) (2023) e2170282 https://doi.org/10.1080/26395940.2023.2170282.

[19] X. Xiao, B.L. Chen, Z.M. Chen, L.Z. Zhu, J.L. Schnoor, Insight into multiple and multilevel structures of biochars and their potential environmental applications: a critical review, Environ. Sci. Technol. 52 (9) (2018) 5027–5047, https://doi.org/10.1021/acs.est.7b06487.

[20] Y. Chen, L. Yang, L. Zhang, J. Li, Y. Zheng, W. Yang, L. Deng, Q. Gao, Q. Mi, X. Li, W. Zeng, X. Ding, H. Xiang, Autotoxins in continuous tobacco cropping soils and their management, Front. Plant Sci. 14 (2023) e1106033, https://doi.org/10.3389/fpls.2023.1106033.

[21] M.D. Xie, W.Q. Chen, X.C. Lai, H.B. Dai, H. Sun, X.Y. Zhou, T.B. Chen, Metabolic responses and their correlations with phytochelatins in Amaranthus hypochondriacus under cadmium stress, Environ. Pollut. 252 (2019) 1791–1800, https://doi.org/10.1016/j.envpol.2019.06.103.

[22] X.Y. Wang, G.Q. Sun, T. Feng, J. Zhang, X. Huang, T. Wang, Z.Q. Xie, X.K. Chu, J. Yang, H. Wang, S.S. Chang, Y.X. Gong, L.F. Ruan, G.Q. Zhang, S.Y. Yan, W. Lian, C. Du, D.B. Yang, Q.L. Zhang, F.F. Lin, J. Liu, H.Y. Zhang, C.R. Ge, S.F. Xiao, J. Ding, M.Y. Geng, Sodium oligomannate therapeutically remodels gut microbiota and suppresses gut bacterial amino acids-shaped neuroinflammation to inhibit Alzheimer's disease progression, Cell Res. 29 (10) (2019) 787–803, https://doi.org/10.1038/s41422-019-0216-x.

[23] C. Hoefer, J. Santner, M. Puschenreiter, W.W. Wenzel, Localized metal solubilization in the rhizosphere of salix smithiana upon sulfur application, Environ. Sci. Technol. 49 (7) (2015) 4522–4529, https://doi.org/10.1021/es505758j.

[24] L. Fu, Y.Z. Ruan, C.Y. Tao, R. Li, Q.R. Shen, Continous application of bioorganic fertilizer induced resilient culturable bacteria community associated with banana Fusarium wilt suppression, Sci. Rep. 6 (2016) e27731, https://doi.org/10.1038/srep27731.

[25] S. Zhang, Z. Gao, H. Liu, Continuous cropping obstacle and rhizospheric microecology. III. Soil phenolic acids and their biological effect, J. Appl. Ecol. 11 (5) (2000) 741–744.

[26] C. Meng, S. Zhang, Y.S. Deng, G.D. Wang, F.Y. Kong, Overexpression of a tomato flavanone 3-hydroxylase-like protein gene improves chilling tolerance in tobacco, Plant Physiol. Biochem. (Issy les Moulineaux, Fr.) 96 (2015) 388–400, https://doi.org/10.1016/j.plaphy.2015.08.019.

[27] Z.Y. Sun, Y.Q. Chen, V. Schaefer, H.M. Liang, W.H. Li, S.Q. Huang, C.L. Peng, Responses of the hybrid between sphagneticola trilobata and sphagneticola calendulacea to low temperature and weak light characteristic in south China, Sci. Rep. 5 (2015) e16906, https://doi.org/10.1038/srep16906.

[28] X.H. Yu, J.X. Juan, Z.L. Gao, Y. Zhang, W.Y. Li, X.M. Jiang, Cloning and transformation of INDUCER of CBF EXPRESSION1 (ICE1) in tomato, Genet. Mol. Res. 14 (4) (2015) 13131–13143, https://doi.org/10.4238/2015.October.26.9.

[29] J. Wang, X. Guo, Adsorption isotherm models: classification, physical meaning, application and solving method, Chemosphere 258 (2020) e127279, https://doi.org/10.1016/j.chemosphere.2020.127279.

[30] Y. Ren, G. Yu, C.P. Shi, L.M. Liu, Q. Guo, C. Han, D. Zhang, L. Zhang, B.X. Liu, H. Gao, J. Zeng, Y. Zhou, Y.H. Qiu, J. Wei, Y.C. n Luo, F.J. Zhu, X.J. Li, Q. Wu, B. Li, W.Y. Fu, Y.L. Tong, J. Meng, Y.H. Fang, J. Dong, Y.T. Feng, S.C. Xie, Q.Q. Yang, H. Yang, Y. Wang, J.B. Zhang, H.D. Gu, H.D. Xuan, G.Q. Zou, C. Luo, L. Huang, B. Yang, Y.C. Dong, J.H. Zhao, J.C. Han, X.L. Zhang, H.S. Huang, Majorbio Cloud: a one-stop, comprehensive bioinformatic platform for multiomics analyses, iMeta 1 (2022) e12, https://doi.org/10.1002/imt2.12.

[31] R. Santhanam, V.T. Luu, A. Weinhold, J. Goldberg, Y. Oh, I.T. Baldwin, Native root-associated bacteria rescue a plant from a sudden-wilt disease that emerged during continuous cropping, P Natl Acad Sci USA 112 (36) (2015) 5013–5020, https://doi.org/10.1073/pnas.1505765112.

[32] L.Y. Zhao, H.L. Guan, R. Wang, H.J. Wang, Z.C. Li, W. Li, P. Xiang, W.M. Xu, Effects of tobacco stem-derived biochar on soil properties and bacterial community structure under continuous cropping of bletilla striata, J. Soil Sci. Plant Nutr. 21 (2) (2021) 1318–1328, https://doi.org/10.1007/s42729-021-00442-y.

[33] S. F. Bender, C. Wagg and M. G. A. van der Heijden, An underground revolution: biodiversity and soil ecological engineering for agricultural sustainability, Trends Ecol. Evol. 31(6) 440-452, https://doi.org/10.1016/j.tree.2016.02.016.

[34] X.M. Zhu, B.L. Chen, L.Z. Zhu, B.S. Xing, Effects and mechanisms of biochar-microbe interactions in soil improvement and pollution remediation: a review, Environ. Pollut. 227 (2017) 98–115, https://doi.org/10.1016/j.envPol.2017.04.032.

[35] Z.T. Ma, Q. Wang, X.W. Wang, X.S. Chen, Y.F. Wang, Z.Q. Mao, Effects of biochar on replant disease by amendment soil environment, Commun. Soil Sci. Plant Anal. 52 (7) (2021) 673–685, https://doi.org/10.1080/00103624.2020.1869758.

[36] C. Liu, R. Xia, M. Tang, X.Y. Liu, R.J. Bian, L. Yang, J.F. Zheng, K. Cheng, X.H. Zhang, M. Drosos, L.Q. Li, S.D. Shan, S. Joseph, G.X. Pan, More microbial manipulation and plant defense than soil fertility for biochar in food production: a field experiment of replanted ginseng with different biochars, Front. Microbiol. 13 (2022) e1065313, https://doi.org/10.3389/fmicb.2022.1065313.

[37] H.H. Zhang, H.L. Feng, C.L. Zhang, X.D. Zhang, W.B. Jin, Z.S. Liang, Identification of phenolic acids in rhizosphere soil of continuous cropping of Bge, Allelopathy J. 53 (2) (2021) 153–163, https://doi.org/10.26651/allelo.j/2021-53-2-1334.

[38] S.S. Sun, R.P. Xue, M.Y. Liu, L.Q. Wang, W. Zhang, Research progress and hotspot analysis of rhizosphere microorganisms based on bibliometrics from 2012 to 2021, Front. Microbiol. 14 (2023) e1085387, https://doi.org/10.3389/fmicb.2023.1085387.

[39] Y. E, M. Jun, H. Haijun, C. Wenfu, Chemical composition and potential bioactivity of volatile from fast pyrolysis of rice husk, J. Anal. Appl. Pyrolysis 112 (2015) 394–400, https://doi.org/10.1016/j.jaap.2015.02.021.

[40] J. Yuan, J. Meng, X. Liang, Y. E, X. Yang, W.F. Chen, Organic molecules from biochar leacheates have a positive effect on rice seedling cold tolerance, Front. Plant Sci. 8 (2017) e1624, https://doi.org/10.3389/fpls.2017.01624.

[41] J. Yuan, J. Meng, X. Liang, E. Yang, X. Yang, W.F. Chen, Biochar's leacheates affect the abscisic acid pathway in rice seedlings under low temperature, Front. Plant Sci. 12 (2021) e646910, https://doi.org/10.3389/fpls.2021.646910.

[42] J. Gao, S. Ge, H. Wang, Y. Fang, L. Sun, T. He, X. Cheng, D. Wang, X. Zhou, H. Cai, C. Li, Y. Liu, Y. E, J. Meng, W. Chen, Biochar-extracted liquor stimulates nitrogen related gene expression on improving nitrogen utilization in rice seedling, Front. Plant Sci. 14 (2023) e1131937, https://doi.org/10.3389/fpls.2023.1131937.

[43] Y. E, J. Meng, H.J. Hu, D.M. Cheng, C.F. Zhu, W.F. Chen, Effects of organic molecules from biochar-extracted liquor on the growth of rice seedlings, Ecotoxicol. Environ. Saf. 170 (2019) 338–345, https://doi.org/10.1016/j.ecoenv.2018.11.108.

[44] T. Ren, H. Wang, Y. Yuan, H. Feng, B. Wang, G. Kuang, Y. Wei, W. Gao, H. Shi, G. Liu, Biochar increases tobacco yield by promoting root growth based on a three-year field application, Sci. Rep. 11 (1) (2021) e21991, https://doi.org/10.1038/s41598-021-01426-9.

[45] J.X. Zhang, Z.F. Zhang, G.M. Shen, R. Wang, L. Gao, Y.C. Dai, T. Zha, J.G. Zhang, Tobacco growth responses and soil properties to rice-straw biochar applied on yellow-brown soil in central China, International Conference on Energy Development and Environmental Protection (2016) 266–273.

[46] H.B. Chen, Y. Feng, X. Yang, B.S. Yang, B. Sarkar, N. Bolan, J. Meng, F.C. Wu, J.W.C. Wong, W.F. Chen, H.L. Wang, Assessing simultaneous immobilization of lead and improvement of phosphorus availability through application of phosphorus-rich biochar in a contaminated soil: a pot experiment, Chemosphere 296 (2022) e133891, https://doi.org/10.1016/j.chemosphere.2022.133891.

[47] H.B. Chen, Y.R. Gao, J.H. Li, C.H. Sun, B. Sarkar, A. Bhatnagar, N. Bolan, X. Yang, J. Meng, Z.Z. Liu, H. Hou, J.W.C. Wong, D.Y. Hou, W.F. Chen, H.L. Wang, Insights into simultaneous adsorption and oxidation of antimonite [Sb(III)] by crawfish shell-derived biochar: spectroscopic investigation and theoretical calculations, Biochar 4 (2022) e37, https://doi.org/10.1007/s42773-022-00161-2.